J Mater Sci: Mater Med (2009) 20:991–999
DOI 10.1007/s10856-008-3656-2

Investigation of polymeric amphiphilic nanoparticles as antitumor drug carriers

Jing Zhang · Xi Guang Chen · Cheng Sheng Liu · Hyun Jin Park

Received: 26 September 2008 / Accepted: 24 November 2008 / Published online: 13 December 2008

Abstract In this paper, polymeric amphiphilic nanoparticles based on oleoyl–chitosan (OCH) with different degrees of substitution (DS, 5%, 11% and 27%) were prepared by Oil/Water emulsification method. Mean diameters of the nanoparticles were 327.4 nm, 255.3 nm and 192.6 nm, respectively. Doxorubicin (DOX) was efficiently loaded into OCH nanoparticles and provided a sustained released after a burst release in PBS. These nanoparticles showed no cytotoxicity to mouse embryo fibroblasts (MEF) and low hemolysis rates (<5%). The results of SDS-PAGE indicated that bovine calf serum (BCS) adsorption on OCH nanoparticles was inhibited by smaller particle size. Cellular uptake was evaluated by incubating fluorescence labeled OCH nanoparticles with human lung carcinoma cells (A549) and mouse macrophages (RAW264.7). Cellular uptake of OCH nanoparticles was time—and concentration—dependent. Finding the appropriate incubation time and concentration of OCH nanoparticles used as drug carriers might decrease phagocytic uptake, increase cancer cell uptake and ultimately improve therapeutic efficiency of antitumor therapeutic agents.

J. Zhang · X. G. Chen (✉) · C. S. Liu
College of Marine Life Science, Ocean University of China, 5# Yushan Road, Qingdao 266003, People's Republic of China
e-mail: xgchen@ouc.edu.cn

H. J. Park
The Graduate School of Biotechnology, Korea University, Seoul 136-701, South Korea
e-mail: hjpark@korea.ac.kr

1 Introduction

Polymeric amphiphiles with both hydrophilic and hydrophobic groups form self-assembled nanoparticles composed of an inner core of hydrophobic segments and an outer shell of hydrophilic segments in aqueous media [1]. Such polymeric particle delivery systems are being used to deliver therapeutic agents like peptides, proteins and polynucleotides [2, 3]. Entrapment in the particles maintains the integrity and activity of these biomolecules, augments the immuno-potentiating effect of the antigens and sometimes modulates the type of antibody response [4, 5].

Recently, various materials have been used for preparing polymeric amphiphilic nanoparticles. Among these materials, chitosan has attracted increasing attention as a non-toxic, hydrophilic, biocompatible, biodegradable and anti-bacterial biomaterial [6–8]. Compared to many other natural polymers, chitosan has positive charge and is mucoadhesive [9]. Therefore, it is used extensively in drug delivery applications [10]. Chitosan-based particulate systems are attracting pharmaceutical and biomedical applications as potential drug delivery devices and widely applied for drug delivery in cancer therapy [11–14].

Drug delivery using polymeric nanoparticles has been recognized as an effective strategy for passive tumor retargeting [1, 15, 16]. It has been reported that many polymeric nanoparticles carriers are suitable for escaping the reticuloendothelial cell system (RES) and renal extraction because of their small particle size ranging approximately from 20 to 100 nm [17]. However, it is also important for nanoparticles carriers to avoid opsonisation. Thus, improving the use of polymeric micelles by overcoming several problems such as low drug entrapment efficiency, short retention time in the tumor site, etc. are still problems. Therefore, it is supported that study of tumor specific accumulation and anti-tumor

effect of larger size nanoparticles can provide important information of the therapeutic potential of the nanoparticles system [1].

When used as drug carriers, understanding the interactions of nanoparticles with blood and cells is crucial for improving their behavior in vivo and in vitro. Therefore, hemolysis and serum protein adsorption seem to be important for the safe use of OCH nanoparticles. The reduction of opsonization is considered as a prerequisite for prolonged blood circulation time [18]. It is reported that nanoparticles have a large surface area/volume ratio and tend to agglomerate and adsorb plasma proteins [19]. Opsonins and other blood proteins could also promote phagocytosis by forming a 'bridge' between the particles and the phagocyte [20].

When nanoparticles agglomerate, or are covered with adsorbed plasma proteins, they are quickly cleared by macrophages before they can reach target cells [21]. The rapid removal of intravenously administered drug carrier systems by the mononuclear phagocytic system (MPS) has been identified as the major obstacle to efficient targeting of particulate drug carriers to target sites such as solid tumors and inflammatory regions in the human body [22, 23]. The main target of many nanoparticle delivery systems is to deliver the drug to the specific cell types, like tumor cells, and is successful only when the drug through its delivery vehicle is internalized into cells [24]. When used as antitumor drug carriers, nanoparticles could act as a drug reservoir through their uptake into cancer cells [25]. Cellular uptake of nanoparticles has been widely investigated [19, 21, 26, 27], however, only a few studies took both phagocytic uptake and cancer cell uptake (both crucial factors for sustained release antitumor drug delivery systems) into consideration.

The aim of the present work was to reveal in vitro drug release, cytotoxicity, hemolysis, serum protein adsorption, and cellular uptake of OCH nanoparticles with different DS (5%, 11% and 27%). In our previous study, oleoyl–chitosan (OCH) nanoparticles with a DS of 11% have been prepared. This kind of nanoparticles is attributed to an extended circulation and contributed to improve therapeutic efficacy [28]. In this study, OCH nanoparticles were prepared by O/W emulsification. The results will provide further information in the design of long circulating biodegradable drug carries with low protein adsorption properties and phagocytic uptake, high cellular uptake by cancer cells and improve the therapeutic activity and safety of antitumor therapeutic agents.

2 Materials and methods

2.1 Materials

Chitosan (DD 82%, Mw 35 KDa), was obtained from Biotech Co. (Mokpo, Korea). Dulbecco's modification of eagle's medium (DMEM), RPMI1640 medium and bovine calf serum (BCS) were obtained from Gibco (AG, Switzerland). Tripolyphosphate sodium (TPP), fluorescein isothiocyanate (FITC) and Triton X-100 were purchased from Sigma (St. Louis, USA). All other reagents and solvents were of analytical grade and used without further purification.

Human blood was supplied by the Affiliated Hospital of Medical College of Qingdao University (Qingdao, China). The pregnant Kunming mouse was purchased from Qingdao Municipal Institute for Drug Control (Qingdao, China). The animal protocol was approved by Shandong Medical Laboratorial Animal Administration Committee. NIH guidelines for the care and use of laboratory animals (NIH Publication #85-23 Rev. 1985) have been observed in the animal experiment.

2.2 Preparation of oleoyl–chitosan (OCH) and FITC-labeled OCH (FITC–OCH)

OCH was prepared by reacting chitosan with oleoyl chloride referenced from Zong [29]. In brief, the OCH with different DS was obtained by controlling the feed ratio of chitosan to oleoyl chloride. OCH I, II and III were with a degree of substitution (DS) of 5%, 11% and 27%, respectively. A mixture of OCH solution (2 mg ml^{-1}, 15 ml) and FITC (2.1 mg) was stirred at room temperature for 24 h, and dialyzed against distilled water using a cellulose membrane (molecular weight cutoff = 8,000–10,000) for 2 days, and lyophilized in a GT 2 freeze-dryer (Leybold AG, Cologne, Germany) after addition of 3% (w/v) mannitol as a cryoprotector. All procedures were carried out under light protection.

2.3 Preparation of self-assembled nanoparticles

Nanoparticles were prepared by O/W emulsification method according to Chen [30]. In brief, methylene chloride (0.45 ml) was added to the OCH or FITC–OCH acetic acid solution (pH 6.5, 200 μg ml^{-1}, 15 ml) while stirring and homogenized (5 min, 14,000×g) for four times. The nanoparticle suspension was held under vacuum for 2 h at 20°C and then sodium tripolyphosphate solution (STPP, 0.25%, 1 ml) was added to the solution while stirring for 1 h. OCH nanoparticles I, II and III were made from OCH with a degree of substitution (DS) of 5%, 11% and 27%, respectively.

DOX–OCH nanoparticles were prepared similarly to that of OCH nanoparticles described above, except that DOX (10 mg) was added to OCH solution (2 mg ml^{-1}, 10 ml) at the beginning of homogenizing. The final FITC–OCH and DOX–OCH nanoparticle suspensions were stored in dark at 20°C for further use.

The zeta potential, particle size and size distributions of OCH nanoparticles were determined by Zatasier NanoZS/ZEN3600 (Malvern Instruments, Herrenberg, Germany). The analysis of particle size and size distributions of OCH nanoparticles were performed at a detector angle of 90 deg, 670 nm, and 25.2°C using samples appropriately diluted with filtrated and double distilled water. The analysis was performed at a temperature of 25.2°C using samples appropriately diluted with NaCl solution in order to maintain a constant ionic strength. All measurements were carried out in triplicate directly after nanoparticle preparation.

2.4 DOX release from DOX–OCH nanoparticles in vitro

The assay was conducted as described by Zhang [28]. Briefly, DOX–OCH nanoparticle suspension (1.5 ml) was placed into a cellulose membrane dialysis tube (molecular weight cutoff = 8,000–10,000). The dialysis tube was placed in 50 ml of release medium (PBS, pH 7.4) and gently shaken in a thermostated shaker bath at 37 ± 0.5°C, 50 rpm for 3 days under light protection. Samples were removed at appropriate intervals and the amount of released DOX was determined using a fluorometer with an emission wavelength of 480 nm and an excitation wavelength of 590 nm in comparison to the standard curve. The accumulative release percentage was calculated.

2.5 Hemolysis test

The hemolysis test was conducted as described by Jumma [31]. In brief, the erythrocyte stock dispersion (100 μl) was added into OCH nanoparticle suspension (1 ml) and incubated under shaking at 100 rpm at 37°C for 0.5–1 h, then the suspension was centrifugated (750×*g*, 5 min). The resulting supernatant (100 μl) was dissolved in a mixture of ethanol and hydrochloric acid, and followed by an additional centrifugation (750×*g*, 3 min). The absorbance of the supernatant was determined at 398 nm. The hemolysis rate (HR %) was calculated with saline solution as negative control (0% lysis) and distilled water as positive control (100% lysis). The experiments were run in triplicate and repeated twice.

2.6 Cytotoxicity test

Mouse embryo fibroblasts (MEF) used in the general cytotoxicity test were obtained through primary culture as described in our previous study [28]. Only cells of 4–7 generations were used in this experiment.

The cell viability was determined using the MTT (3-(4, 5-dimethylthiazolyl-2)-2, 5-diphenyltetrazolium bromide) method. Briefly, MEF at logarithmic growth phase were added to 96-well culture plates (5×10^4 cells/ml, 100 μl/well) and incubated overnight. The culture medium was then replaced with the appropriate OCH nanoparticle suspension (200 μl/well, 25 μg ml^{-1} to 800 μg ml^{-1} in culture medium, pH 6.5) and incubated at 37°C, 5% CO_2 and 95% relative humidity for 1 day. The negative control was blank culture medium. The percent of viability was expressed as relative growth rate (RGR %) by

$$\text{RGR } \% = \frac{D_t}{D_{nc}} \times 100\%$$

where D_t and D_{nc} are the absorbances of the tested sample and the negative control at 570 nm.

2.7 Protein adsorption assay

The adsorption of bovine calf serum (BCS) proteins to OCH nanoparticles was studied at pH 6.5. Nanoparticle suspension (100 μg ml^{-1}, 1 ml) was incubated in fresh BCS (1%, v/v, 1 ml) for 0.5 h at 37°C, then separated by ultracentrifugation (Beckman Instruments Inc., Palo Alto, CA) at 40,000×*g* for 15 min at 4°C and extensively washed three times with distilled water (1 ml) to remove proteins not firmly adsorbed onto nanoparticle surface. The adsorbed proteins were desorbed from the surface of the OCH nanoparticles by PBS containing 1% SDS [19] and applied to the SDS-PAGE. The SDS-PAGE was performed on an acrylamide gel consisting of 10% separating gel and 5% stacking gel under reducing conditions. The protein was visualized by staining with Coomassie Brilliant Blue R-250.

2.8 Uptake of FITC–OCH nanoparticles by A549 and RAW264.7

Human lung carcinoma cell line A549 and mouse macrophage cell line RAW264.7 were routinely cultured in RPMI-1640 medium, supplemented with 10% fetal calf serum (FCS), 100 U ml^{-1} penicillin, and 100 U ml^{-1} streptomycin at 37°C, 5% CO_2 and 95% relative humidity [21].

The quantitative study of cellular uptake in vitro was investigated similarly to Win et al. [32]. In brief, cells were transferred to 96-well culture plates (3×10^4 cells/ml, 100 μl/well) and incubated for 24 h to form a confluent monolayer. The culture medium was then replaced by transport buffer (Hank's balanced salt solution, HBSS, pH 7.4) and pre-incubated at 37°C for 30 min. Then the transport medium was changed with 100 μl of freshly prepared FITC–OCH nanoparticle suspension (25 μg ml^{-1} to 400 μg ml^{-1} in HBSS) and incubated at 37°C for 0.5–4 h. After the incubation, the cell monolayer was washed three times with ice-cold phosphate-buffered saline (PBS, pH 7.4) and Triton X-100 (0.5%, in 0.2 N NaOH)

was added. Cell-associated FITC–OCH nanoparticles were quantified by analyzing the cell lysate in a fluorescence plate reader (Bio-Tek Instruments, USA, λex 485 nm, λem 528 nm). Cellular uptake efficiency was expressed by the ratio of the amount of FITC associated with cells to the total amount of FITC present in the feed nanoparticle suspension.

To study cellular uptake via fluorescence microscopy, cell suspension (4×10^5 cells/ml, 1 ml/well) were cultured in 6-well cultureplates containing 18 mm coverslips for 24 h. Then the culture medium was replaced by HBSS and pre-incubated at 37°C for 0.5 h, and then changed with FITC–OCH nanoparticle suspension (200 μg ml^{-1} in HBSS). After 0.5–4 h of incubation at 37°C, the cells were washed three times with ice-cold PBS, and the coverslips were put on slides and viewed by fluorescence microscopy (Olympus, Japan).

2.9 Statistical analyses

All data were presented as mean ± standard deviation (±SD). Difference between groups was evaluated using one paired Student's *t*-test. P value < 0.05 was considered statistically significant. Calculations were done using the software SigmaPlot 10.0.

3 Results and discussion

3.1 Characterization of OCH nanoparticles

The particle size and distributions of OCH nanoparticles was shown in Fig. 1. The mean diameter was 327.4 nm, 255.3 nm and 192.6 nm, respectively. The zeta potential of OCH nanoparticles was shown in Table 1. The results indicated that zeta potential of OCH nanoparticles decreased from 23.7 mV to 15.5 mV with the increase of DS. Since free amino groups of chitosan were responsible for the measured positive zeta potential values, the results might be related with higher degree of substitution of OCH which decreased the amount of primary amino groups on the surface of OCH nanoparticles.

3.2 Drug release in vitro

In this study, doxorubicin (DOX) was incorporated into OCH nanoparticles. DOX is a well-known anticancer drug, however, it is hydrophobic and possesses inevitable, serious side effects such as nonspecific toxicity that limit the dose and use of the drug. In our previous study, DOX was successfully entrapped into DOX–OCH nanoparticles II, and the nanoparticles had a high EE % of DOX [28].

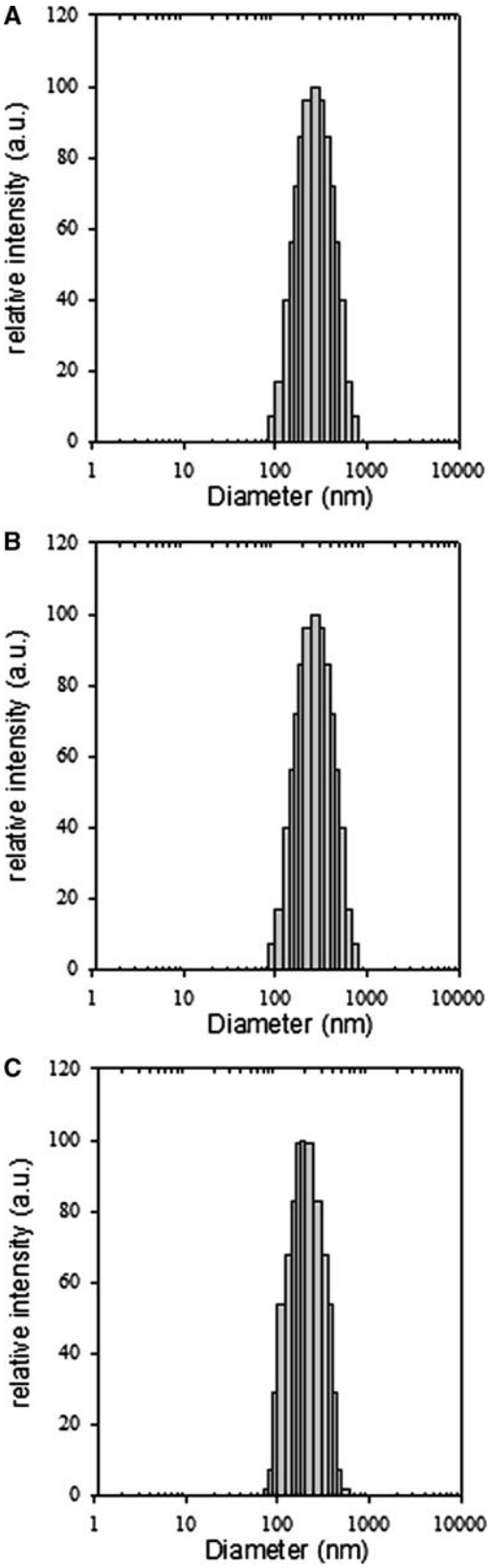

Fig. 1 Distribution of nanoparticles in number ($\theta = 90°$; $\lambda = 670$ nm; $T = 25.2$°C). **a** OCH nanoparticles I. **b** OCH nanoparticles II. **c** OCH nanoparticles III

Table 1 Zeta potential of OCH nanoparticles degree of substitution (DS) of oleoyl–chitosan (OCH) and zeta potential of OCH nanoparticles

Nanoparticles	DS (%)	Zeta potential (mV)
OCH nanoparticle I	5	23.7 ± 0.9
OCH nanoparticle II	11	18.9 ± 0.7
OCH nanoparticle III	27	15.5 ± 0.6

Data represented the mean ± SD, $n = 3$

DS = number of oleic acid groups per 100 anhydroglucose units of chitosan (%)

The release of doxorubicin from DOX–OCH nanoparticles I, II and III in PBS (pH 7.4) in vitro was represented in Fig. 2. There was a burst release for 8 h, followed by a sustained release until 72 h. 79.01%, 72.77% and 69.15% of DOX was released from OCH nanoparticles I, II and III for 3 days, respectively. The results suggested that the DOX not incorporated into OCH nanoparticles and located onto the surface of nanoparticles could be detected in the release media within 8 h, and after 8 h, the nanoparticles might act as a barrier against the release of DOX located in the hydrophobic core of nanoparticles. The hydrolysis and the migration of DOX to release media might be strongly restricted by the hydrophobic core of the nanoparticles [1]. Nanoparticles based on OCH with higher degree of substitution showed higher sustained release efficacy, which might because that the increase of hydrophobic groups facilitated the formation and stability of OCH nanoparticles and enhanced the affinity between DOX and nanoparticles, thus decreased the burst of drug release. These results indicated that OCH nanoparticles could contribute to an extended circulation of DOX and therefore improved therapeutic efficacy. Based on the stability data, the release

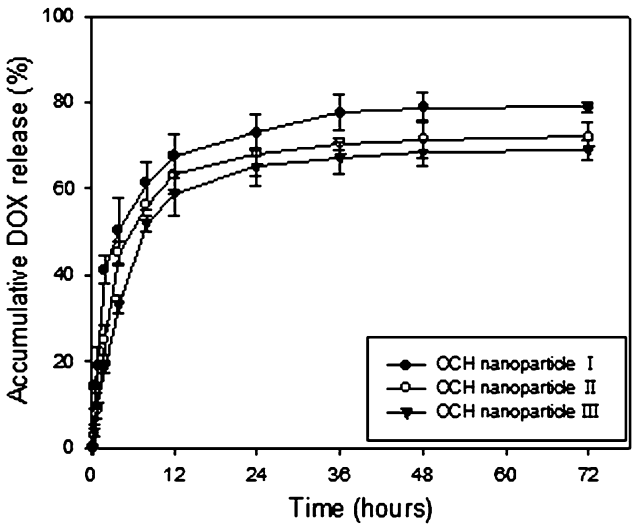

Fig. 2 In vitro DOX release from DOX–OCH nanoparticles in PBS, pH 7.4. Data represented the mean ± SD, $n = 3$

of DOX from DOX–OCH nanoparticles might be controlled by diffusion as a result of partitioning between the core and the aqueous phase, because DOX–OCH nanoparticles are stable in aqueous environment for 7 days.

3.3 Hemolysis test

Hemolysis of the blood is the problem associated with bioincompatibility [33, 34]. Hemolysis rates (HR %) of human fresh blood with OCH nanoparticle I, II and III was shown in Table 2. Hemolytic activity of OCH nanoparticle I, II and III all slightly increased with particle concentration and incubation time. It was speculated that it took time for OCH nanoparticles to contact and act with RBCs, and the membrane of RBCs could be damaged only if there were enough polymeric amphiphiles acting with them [28]. At the same incubation time and concentration, the HR % varied as follows: OCH nanoparticle I > II > III ($P < 0.05$). Previous studies indicated that chitosan promoted surface induced hemolysis, which can be attributed in part to the electrostatic interactions [35, 36]. Thus the different hemolytic activity could be attributed to the different positive zeta potential values of OCH nanoparticles. HR % of OCH nanoparticles at different concentration and time was below 5, respectively, which was regarded as non-toxic effect level according to Rao [37]. It should be emphasized that only the requisite concentration of OCH nanoparticles be used to avoid additional hemolysis.

3.4 Cytotoxicity test

In order to further prove the safety of OCH nanoparticles as drug carriers, we evaluated their cytotoxicity to MEF proliferation over a range of concentrations (25 μg ml^{-1} to 800 μg ml^{-1}). As shown in Fig. 3, there were no significant differences between the absorbance of the negative control and the wells treated with OCH nanoparticles I, II, III at each concentration ($P > 0.05$), except that it stimulated the growth of MEF at low concentration (50, 100 μg ml^{-1}) of OCH nanoparticle I and high concentration (400, 800 μg ml^{-1}) of OCH nanoparticle II ($P < 0.05$). Thus, all types of OCH nanoparticles showed no cytotoxicity and were appropriate to be drug carriers.

3.5 Protein adsorption analysis

When blood is in contact with a foreign material surface, firstly, the adsorption of plasma proteins occurs [34]. To examine the specific interactions of protein with the OCH nanoparticles, adsorption for BCS was studied using SDS-PAGE. Figure 4 showed proteins adsorption on OCH nanoparticles I, II and III from 1% BCS. It could be concluded by comparing the proteins on OCH nanoparticles

Table 2 Hemolysis rate (HR %) of OCH nanoparticles

Sample		OCH nanoparticle I		OCH nanoparticle II		OCH nanoparticle III	
		1 mg ml^{-1}	2 mg ml^{-1}	1 mg ml^{-1}	2 mg ml^{-1}	1 mg ml^{-1}	2 mg ml^{-1}
HR %	30 min	1.58 ± 0.15	2.58 ± 0.30	1.32 ± 0.11	2.39 ± 0.06	1.09 ± 0.10	2.15 ± 0.19
	60 min	1.93 ± 0.03	3.76 ± 0.16	1.77 ± 0.11	3.06 ± 0.12	1.51 ± 0.25	2.89 ± 0.17

Data represented the mean ± SD, $n = 3$

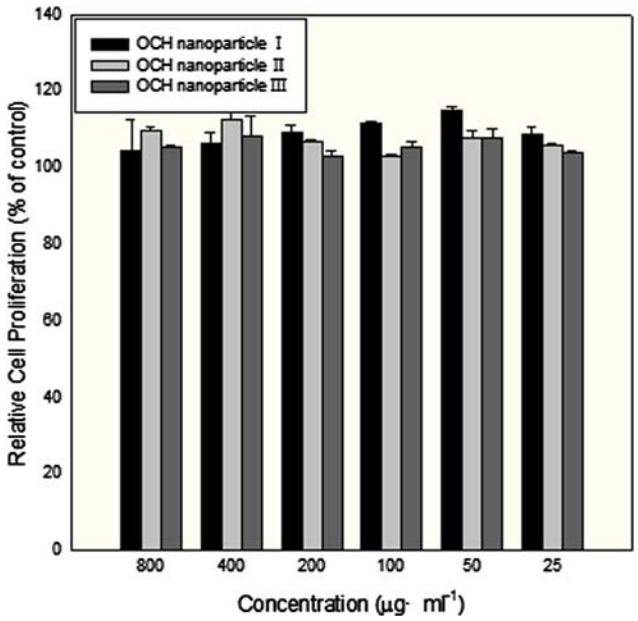

Fig. 3 In vitro cytotoxicity of OCH nanoparticles in MEF. Data represented the mean ± SD, $n = 6$

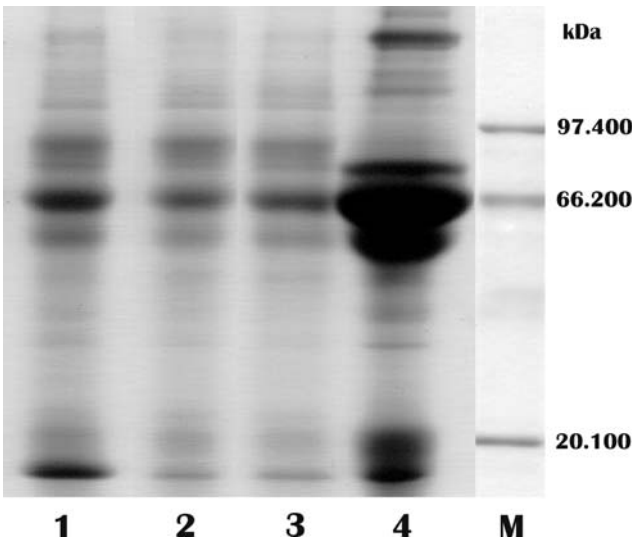

Fig. 4 SDS-PAGE electrophoresis gel stained by Coomessie Blue. Lane M, maker; Lane 1, serum proteins adsorbed on OCH nanoparticle I; Lane 2, serum proteins adsorbed on OCH nanoparticle II; Lane 3, serum proteins adsorbed on OCH nanoparticle III; Lane 4, 1% BCS before adsorption

(lane 1–3) to the BCS (lane 4) that the surface of OCH nanoparticle I, II and III bound certain amount of proteins, and the amount of BSA (67.000 kDa) was especially high. It was also shown that the amount of serum proteins adsorbed decreased with particle size. This might be responsible of differences in terms of degree of substitution among OCH nanoparticle I, II and III. When the primary amino groups at the 2-position was substituted with oleoyl, the positive charges on the surface of chitosan decreased. Thus the zeta potential of OCH nanoparticles decreased and weakened the static attraction between proteins and nanoparticles. Folding of the OCH chains on the surface of nanoparticles was also likely a reason for the different protein adsorption results. This folding leaded to the formation of coils including water molecules [27], and therefore decreased the adsorbing of proteins onto particle surface.

3.6 Cellular uptake of FITC–OCH nanoparticles

OCH nanoparticle III was applied in the cellular uptake study since it showed lower hemolysis and protein adsorption, and higher drug release efficacy in the forementioned research. Uptake of FITC–OCH nanoparticles by both human lung carcinoma cells (A549) and mouse macrophages (RAW264.7) were investigated in this study. Before the study of cellular uptake, the cytotoxicity of FITC–OCH nanoparticles on cells was assessed by MTT assay. The MTT test indicated FITC–OCH nanoparticle at the concentration of lower than 400 μg ml^{-1} did not cause cytotoxicity to A549 and RAW264.7 within 4 h (data not shown). This result ensured that, under 400 μg ml^{-1}, cellular uptake of nanoparticles was not associated with their cytotoxicity.

As shown in Fig. 5, an obviously time-dependent increased uptake was observed for FITC–OCH nanoparticles from 0.5 to 4 h. For RAW264.7, cellular uptake increased rapidly after 1 h incubation. For A549 cells, the uptake of FITC–OCH nanoparticles increased rapidly with the incubation time over 2 h, whereas the increase of cellular uptake became slower beyond 2 h of incubation. This phenomenon could be due to the limited saturation level. However, it should be emphasized that the cellular uptake of nanoparticles by A549 cells was higher than that of RAW264.7 cells beyond 2 h of incubation.

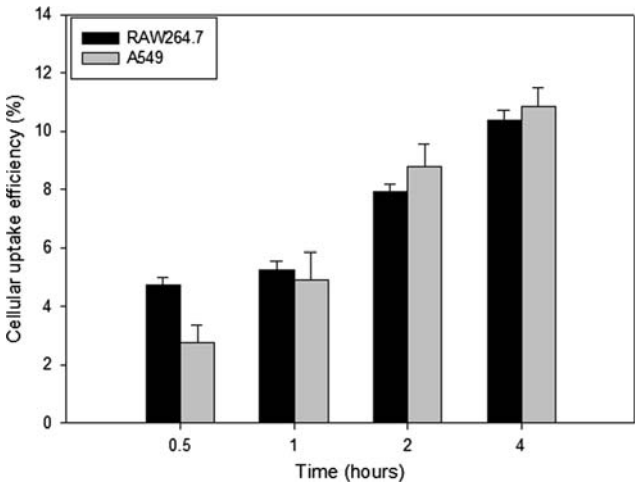

Fig. 5 Cellular uptake efficiency (%) of FITC–OCH nanoparticles with a particle concentration of 200 μg/ml at 37°C. Data represented the mean ± SD, $n = 3$

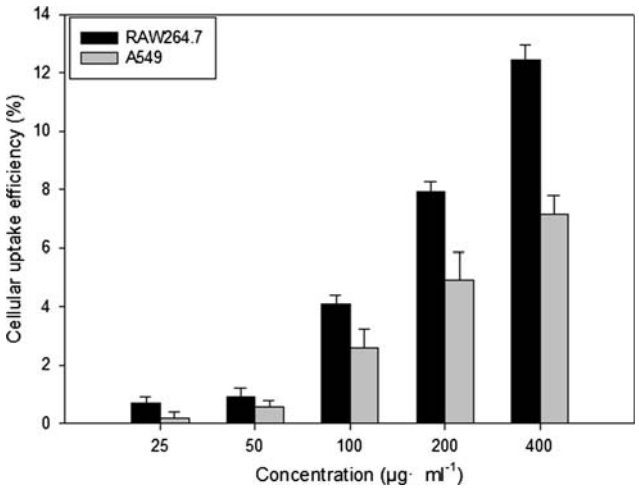

Fig. 6 Cellular uptake efficiency (%) of FITC–OCH nanoparticles after 2 h incubation at 37°C. Data represented the mean ± SD, $n = 3$

The results in Fig. 6 suggested that cellular uptake of FITC–OCH nanoparticles was significantly influenced by concentration. The uptake by both kinds of cells increased with particle concentration in the medium after 2 h incubation. No saturation behavior was obtained, indicating their potential ability to be drug carriers. There was no significant cellular uptake by A549 cells at a low particle concentration of 25 μg ml^{-1}, which indicated that the nanoparticle concentration should reach a certain level to initiate the cellular uptake.

The uptake of the FITC–OCH nanoparticles by A549 and RAW264.7 cells with incubation time of 1–4 h was visualized using fluorescence microscopy. The effect of incubation time on the cellular uptake was clearly evidenced in Fig. 7. It strongly supported the previous

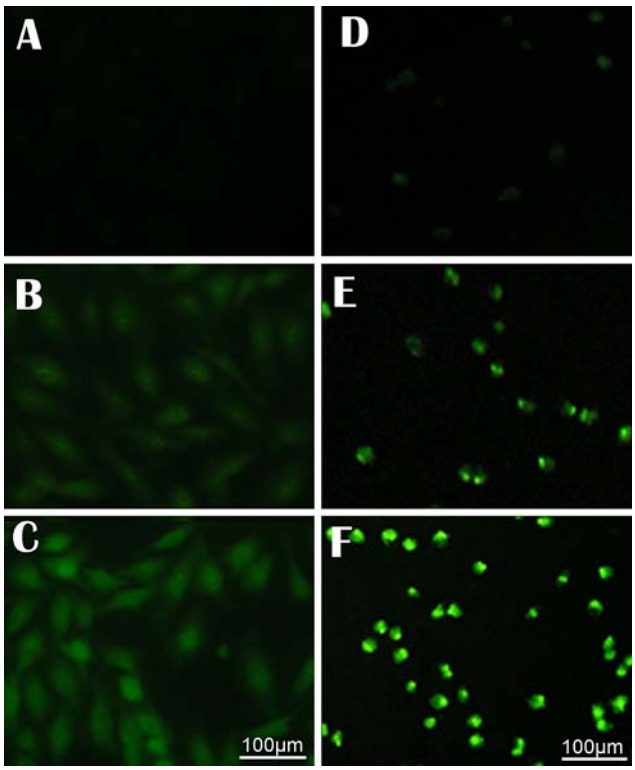

Fig. 7 Fluorescence microscopic images of A549 cells and RAW264.7 cells incubated with FITC–OCH nanoparticles with a concentration of 200 μg ml^{-1} at 37°C: **a** A549 cells, after 1 h incubation. **b** A549 cells, after 2 h incubation. **c** A549 cells, after 4 h incubation. **d** RAW264.7 cells, after 1 h incubation. **e** RAW264.7 cells, after 2 h incubation. **f** RAW264.7 cells, after 4 h incubation

quantitative measurement by showing stronger fluorescence in the cells with the increase of incubation time. Fluorescence was not detected in control cells that had not been exposed to the FITC–OCH nanoparticles.

It has been demonstrated that particle size is a key factor on cellular uptake of nanoparticles [26, 27], thus OCH nanoparticle III (192.6 nm) was chosen to investigate the capability of nanoparticles to be drug carriers in vitro. The introduction of the concept "the enhanced permeability and retention" (EPR) effect [38] to cancer chemotherapy gives rise to extensive research on polymeric drug carriers. A strategy of drug delivery systems using the EPR effect is to use polymeric micelles as long-circulating drug carriers. The reduction of phagocytosis, mechanical filtration and levels of opsonisation are also considered as factors that affect prolonged blood circulation time. The accumulation and uptake of nanoparticles by cancer cells is also generally considered as an important requirement for therapeutic application of antitumor drug delivery systems. The results shown in Figs. 5 and 6 indicated that uptake efficiency of nanoparticles by A549 cells and by RAW264.7 varied with incubation time and particle concentration. It could be speculated that finding an appropriate concentration of

OCH nanoparticles was crucial to the initiation of cellular uptake. Finding an appropriate incubation time and particle concentration could decrease phagocytic uptake and increase cancer cell uptake in vitro. These results indicated that OCH nanoparticles might improve therapeutic efficiency of antitumor drugs. However, further study in vivo still needed.

4 Conclusions

In this study, cytotoxicity, hemolysis, serum protein adsorption and cellular uptake properties of OCH nanoparticles based on OCH with different degree of substitution were investigated in vitro. OCH nanoparticles with a low degree of substitution showed no detected cytotoxicity, high sustained drug release efficacy and low serum proteins adsorption, therefore exhibited great potential to be antitumor drug carriers. These effects might be related to the inclusion of a higher density of oleoyl groups that facilitated the formation and stability of OCH nanoparticles, and the decrease of positive zeta potential values that weakened the interaction between nanoparticles and proteins. The nanoparticles could be taken up by cells, and the levels of binding and uptake increased with particle concentration and incubation time. The information provided in this study would be valuable for the development of a sustained release drug delivery based on polymeric amphiphilic nanoparticles for the aim of tumor therapy.

Acknowledgements This work was supported by grants from national natural science foundation of China (NSFC, 30770582) and international science and technology cooperation project (ISTCP, 2008DFA31640).

References

1. Y.J. Son, J.S. Jang, Y.W. Cho, H. Chung, R.W. Park, I.C. Kwon, I.S. Kim, J.Y. Park, S.B. Seo, C.R. Park, S.Y. Jeong, J. Control. Release **91**, 135 (2003). doi:10.1016/S0168-3659(03)00231-1
2. G. Sandri, M.C. Bonferoni, S. Rossi, F. Ferrari, S. Gibin, Y. Zambito, G. Di Colo, C. Caramella, Eur. J. Pharm. Biopharm. **65**, 68 (2007). doi:10.1016/j.ejpb.2006.07.016
3. A. Maruyama, T. Ishihara, J.S. Kim, S.W. Kim, T. Akaike, Colloids Surf. A Physicochem. Eng. Asp. **153**, 439 (1999). doi:10.1016/S0927-7757(98)00534-2
4. T. Madan, N. Munshi, T.K. De, A. Maitra, P.U. Sarma, S.S. Aggarwal, Int. J. Pharm. **159**, 135 (1997). doi:10.1016/S0378-5173(97)00278-0
5. N. Arora, S.V. Gangal, Efficacy of liposome entrapped allergen in down-regulation of IgE response in mice. Clin. Exp. Allergy **22**, 35 (1992). doi:10.1111/j.1365-2222.1992.tb00112.x
6. K.E. Crompton, J.D. Goud, R.V. Bellamkonda, T.R. Gengenbach, D.I. Finkelstein, M.K. Horne, J.S. Forsythe, Biomaterials **28**, 441 (2007). doi:10.1016/j.biomaterials.2006.08.044
7. N.V. Majeti, K. Ravi, React. Funct. Polym. **46**, 1 (2000). doi:10.1016/S1381-5148(00)00038-9
8. L. Illum, I. Jabbal-Gill, M. Hinchcliffe, A.N. Fisher, S.S. Davis, Adv. Drug Deliv. Rev. **51**, 81 (2001). doi:10.1016/S0169-409X(01)00171-5
9. V. Dodane, K.M. Amin, J.R. Merwin, Int. J. Pharm. **182**, 21 (1999). doi:10.1016/S0378-5173(99)00030-7
10. A.K. Bajpai, S.K. Shukla, S. Bhanu, S. Kankane, Prog. Polym. Sci (in press)
11. S.A. Agnihotri, N.N. Mallikarjuna, T.M. Aminabhavi, J. Control. Release **100**, 5 (2004). doi:10.1016/j.jconrel.2004.08.010
12. H. Tokumitsu, H. Ichikawa, Y. Fukumori, Pharm. Res. **16**, 1830 (1999). doi:10.1023/A:1018995124527
13. S. Mitra, U. Gaur, P.C. Ghosh, A.N. Maitra, J. Control. Release **74**, 317 (2001). doi:10.1016/S0168-3659(01)00342-X
14. J.H. Kim, Y.S. Kim, S. Kim, J.H. Park, K. Kim, K. Choi, H. Chung, S.Y. Jeong, R.W. Park, I.S. Kim, I.C. Kwon, J. Control. Release **111**, 228 (2006). doi:10.1016/j.jconrel.2005.12.013
15. M. Pechar, K. Ulbrich, V. šubr, L.W. Seymour, E.H. Schacht, Bioconjug. Chem. **11**, 131 (2000). doi:10.1021/bc990092l
16. G.S. Kwon, M. Naito, M. Yokoyama, T. Okano, Y. Sakurai, K. Kataoka, J. Control. Release **48**, 195 (1997). doi:10.1016/S0168-3659(97)00039-4
17. H.S. Yoo, T.G. Park, J. Control. Release **70**, 63 (2001). doi:10.1016/S0168-3659(00)00340-0
18. T. Ameller, V. Marsaud, P. Legrand, R. Gref, G. Barratt, J.M. Renoir, Pharm. Res. **20**, 1063 (2003). doi:10.1023/A:1024418524688
19. C. Fang, B. Shi, Y.Y. Pei, M.H. Hong, J. Wu, H.Z. Chen, Eur. J. Pharm. Sci. **27**, 27 (2006). doi:10.1016/j.ejps.2005.08.002
20. M.T. Peracchia, S. Harnisch, H. Pinto-Alphandary, A. Gulik, J.C. Dedieu, D. Desmaële, J. d' Angelo, R.H. Müller, P. Couvreur, Biomaterials **20**, 1269 (1999). doi:10.1016/S0142-9612(99)00021-6
21. Y. Zhang, N. Kohler, M.Q. Zhang, Biomaterials **23**, 1553 (2002). doi:10.1016/S0142-9612(01)00267-8
22. S.E. Dunn, A.G.A. Coombes, M.C. Garnett, S.S. Davis, M.C. Davies, L. Illum, J. Control. Release **44**, 65 (1997). doi:10.1016/S0168-3659(96)01504-0
23. V.C.F. Mosqueira, P. Legrand, J.L. Morgat, M. Vert, E. Mysiakine, R. Gref, J.P. Devissaguet, G. Barratt, Pharm. Res. **18**, 1411 (2001). doi:10.1023/A:1012248721523
24. R. Wattiaux, N. Laurent, S.W. Conninck, M. Jadot, Adv. Drug Deliv. Rev. **41**, 201 (2000). doi:10.1016/S0169-409X(99)00066-6
25. A. Lamprecht, J.P. Benoit, J. Control. Release **112**, 208 (2006). doi:10.1016/j.jconrel.2006.02.014
26. I. Brigger, C. Dubernet, P. Couvreur, Adv. Drug Deliv. Rev. **54**, 631 (2002). doi:10.1016/S0169-409X(02)00044-3
27. R. Gref, M. Lück, P. Quellec, M. Marchand, E. Dellacherie, S. Harnisch, T. Blunk, R.H. Müller, Colloids Surf. B Biointerfaces **18**, 301 (2000). doi:10.1016/S0927-7765(99)00156-3
28. J. Zhang, X.G. Chen, Y.Y. Li, C.S. Liu, Nanomedicine **3**, 258 (2007). doi:10.1016/j.nano.2007.08.002
29. Z. Zong, Y. Kimura, M. Takahashi, H. Yamane, Polymer Guildf **41**, 899 (2000). doi:10.1016/S0032-3861(99)00270-0
30. X.G. Chen, C.M. Lee, H.J. Park, J. Agric. Food. Chem. **51**, 3135 (2003). doi:10.1021/jf0208482
31. M. Jumma, F.H. Furkert, B.W. Müller, Eur. J. Pharm. Biopharm. **53**, 115 (2002). doi:10.1016/S0939-6411(01)00191-6
32. K.Y. Win, S.S. Feng, Biomaterials **26**, 2713 (2005). doi:10.1016/j.biomaterials.2004.07.050
33. D. Shim, D.S. Wechsler, T.R. Lloyd, R.H. Beekman III, Cathet. Cardiovasc. Diagn. **39**, 287 (1996). doi:10.1002/(SICI)1097-0304(199611)39:3<287::AID-CCD17>3.0.CO;2-C
34. Q.Z. Wang, X.G. Chen, Z.X. Li, S. Wang, C.S. Liu, X.H. Meng, C.G. Liu, Y.H. Lv, L.J. Yu, J. Mater. Sci. Mater. Med. **19**, 1371 (2008). doi:10.1007/s10856-007-3243-y

35. S. Hirano, M. Zhang, M. Nakagawa, T. Miyata, Biomaterials **21**, 997 (2000). doi:10.1016/S0142-9612(99)00258-6
36. M.M. Amiji, Colloids Surf. B Biointerfaces **10**, 263 (1998). doi: 10.1016/S0927-7765(98)00005-8
37. S.B. Rao, C.P. Sharma, J. Biomed. Mater. Res. **34**, 21 (1997). doi:10.1002/(SICI)1097-4636(199701)34:1<21::AID-JBM4>3.0.CO;2-P
38. Y. Matsumura, H. Maeda, Cancer Res. **46**, 6387 (1986)